

# Modeling and Analysis of Cascade Multilevel PWM Rectifier Using Circuit DQ Transformation

Nam-Sup Choi, Member, KIMICS

**Abstract**— This paper presents a cascade multilevel PWM rectifier without the isolation transformers for energy build-up at each inverter modules. The features and advantages of the proposed PWM rectifier can be summarized as follows; 1) It realizes the high power high voltage AC/DC power conversion, 2) It uses no transformer which is bulky and heavy, 3) It has hybrid structure so that switching devices can be effectively utilized, 4) It produces high quality AC current even in high power high voltage applications, 5) The input power factor remains unity by simple modulation index control. The multilevel rectifier is analyzed by using the circuit DQ transformation whereby the characteristics and control equations are obtained. Finally, it will be shown that the system simulation reveals the validity of analyses.

**Index Terms**—Circuit DQ Transformation, Multilevel Inverter, PWM Rectifier, Unity Power Factor

## I. INTRODUCTION

The three phase PWM rectifier has been widely studied and used as an excellent AC/DC power converter. The PWM rectifier has superior advantages over phase controlled rectifier(PCR) such as sinusoidal input current, adjustable power factor, better DC output voltage etc. In high voltage and high power applications, however, such features of the PWM rectifier may be deteriorated because of lack of high frequency switching device endurable to high voltage and/or high power [1-2].

Nowadays, one of the practical solutions to cope with high voltage and/or high power application is to employ so called multilevel PWM converter. Up to date, three major types of multilevel structure have been reported; diode-clamped type, flying-capacitor type, cascade type. Considering the multilevel converters as a rectifier, 1) the diode-clamped type has drawback of DC voltage unbalancing problem, 2) the flying-capacitor type needs large number of capacitors and the complicated control, 3) the cascade type has simple modular structure of proven technology but it is supposed to have separate DC sources, and thus isolation transformers, to synthesize multilevel output [3-7].

This paper proposes a cascade multilevel PWM rectifier without bulky and heavy isolation transformers. It will

be seen that the DC voltages required to make multilevel output may be built up from AC utility source while the input power factor remains unity. Moreover, the proposed rectifier has hybrid structure. So, for example, GTO, high power low speed switch, is involved in high power low frequency module and IGBT, low power high speed switch, in low power high frequency module.

The proposed multilevel PWM rectifier is analyzed by using the circuit DQ transformation[1],[7] whereby the characteristic and operating control equations are obtained with ease. Finally, such advantages and characteristics of the rectifier will be verified through PSIM simulations.

## II. SYSTEM OVERVIEW

Fig. 1 shows the proposed cascade multilevel PWM rectifier. The rectifier consists of three full bridge(FB) inverters using IGBT switches and a three phase(TP) inverter composed of GTO devices. The FB inverters operated at high switching frequency may have lower power rating than that of the TP inverter operated at lower switching frequency and this hybrid structure enables the switching devices to be fully utilized with synergism.

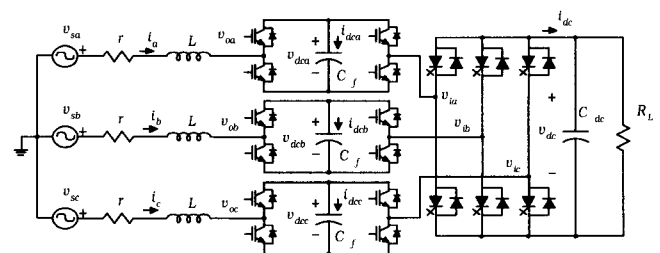


Fig. 1 Cascade 5-level PWM rectifier.

Assuming symmetry operation, there are four effective control variables; modulation index( $m_1$ ) and control angle( $\alpha_1$ ) for FB inverters and modulation index( $m_2$ ) and control angle( $\alpha_2$ ) for TP inverter, where  $\alpha_1$ ,  $\alpha_2$  are with respect of the angle of utility source voltage. Adjusting such control variables, the DC voltages of FB inverters used for multilevel output synthesis can be build up without any separate charging/discharging circuitry. For 5-level output voltage, the relationship between the DC voltages of FB inverter,  $v_{dcf}$  and TP inverter,  $v_{dc}$  will be controlled as given by

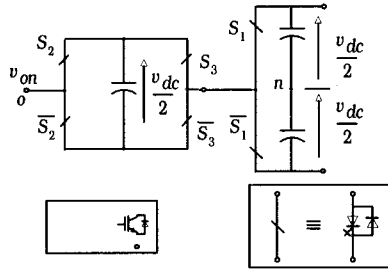
$$v_{dcf} = \frac{v_{dc}}{2} \quad (1)$$

Fig. 2 shows the switching table for the cascade multilevel PWM rectifier. As seen in the switching table, there are some redundancy to produce the same output voltage,  $v_{on}$ . The source voltages with angular speed,  $\omega$  are assumed ideal and balanced and are given as follows:

$$\mathbf{v}_{s,abc} = [v_{sa} \ v_{sb} \ v_{sc}]^T = \sqrt{\frac{2}{3}} \cdot V_s \mathbf{SIN}(\omega t) \quad (2)$$

where  $V_s$  is the rms line-to-line AC source voltage and  $T$  represents the transpose of matrix.

$$\mathbf{SIN}(\omega t) = \begin{bmatrix} \sin(\omega t) \\ \sin(\omega t - 2\pi/3) \\ \sin(\omega t + 2\pi/3) \end{bmatrix} \quad (3)$$



$v_{on}$	$v_{dc}$	$v_{dc}/2$	0	$-v_{dc}/2$	$-v_{dc}$
$S_1$	on	on	on	off	off
$S_2$	on	on	off	on	off
$S_3$	off	on	off	off	on

Fig. 2 Switching table.

### III. CIRCUIT DQ TRANSFORMATION

The original circuit is too complex to analyze, so it is partitioned into several basic subcircuits as shown in Fig. 3. By using circuit DQ transformation, the rotational three-phase circuit shown in Fig. 1 is transformed into the stationary linear time-invariant (LTI) circuit. Note that the only fundamental component in the currents and voltages is considered to focus on the basic features of the circuit [7].

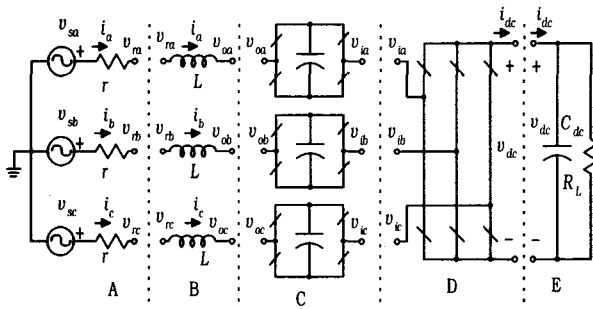


Fig. 3 Circuit partitioning.

The power invariant DQ transformation matrix  $\mathbf{K}$  is given by

$$\mathbf{K} = \sqrt{\frac{2}{3}} \begin{bmatrix} \mathbf{COS}^T(\omega t + \alpha_1) \\ \mathbf{SIN}^T(\omega t + \alpha_1) \\ \mathbf{I}^T/\sqrt{2} \end{bmatrix}, \quad \mathbf{I}^T = [1 \ 1 \ 1]^T \quad (4)$$

A variable  $\mathbf{x}_{abc}$  that denotes any AC voltages and currents is transformed into  $\mathbf{x}_{qdo}$  by DQ transformation matrix  $\mathbf{K}$

$$\mathbf{x}_{qdo} = \mathbf{K} \mathbf{x}_{abc} \quad (5)$$

The voltage-current relationships in the resistor-inductor set gives

$$\mathbf{v}_{s,abc} = r \mathbf{i}_{abc} + \mathbf{v}_{r,abc} \quad (\text{part A}) \quad (6)$$

$$L \frac{d}{dt} \mathbf{i}_{abc} = \mathbf{v}_{r,abc} - \mathbf{v}_{o,abc} \quad (\text{part B}). \quad (7)$$

Assuming symmetry operation of each FB inverters,

$$v_{dca} \cong v_{dcb} \cong v_{dcc} \cong v_{def} \quad (8)$$

$$i_{dca} \cong i_{dcb} \cong i_{dcc} \cong i_{def} \quad (9)$$

The voltage-current relationships in part C becomes

$$\mathbf{v}_{o,abc} - \mathbf{v}_{i,abc} = \sqrt{\frac{2}{3}} d_1 \cdot \mathbf{SIN}(\omega t + \alpha_1) v_{def} \quad (10)$$

$$3i_{def} = \sqrt{\frac{2}{3}} d_1 \cdot \mathbf{SIN}^T(\omega t + \alpha_1) \mathbf{i}_{abc} \quad (11)$$

where  $d_1$  is associated with a modulation index of FB inverters, that is

$$d_1 = \sqrt{\frac{3}{2}} m_1 \quad (12)$$

In part D, the following equations are obtained considering the only fundamental components,

$$\mathbf{v}_{i,abc} = \sqrt{\frac{2}{3}} d_2 \cdot \mathbf{SIN}(\omega t + \alpha_2) v_{dc} \quad (13)$$

$$i_{dc} = \sqrt{\frac{2}{3}} d_2 \cdot \mathbf{SIN}^T(\omega t + \alpha_2) \mathbf{i}_{abc} \quad (14)$$

where  $d_2$  indicates the modulation index of TP inverter such that,

$$d_2 = \sqrt{\frac{8}{3}} m_2 \quad (15)$$

Now, applying the matrix  $\mathbf{K}$  to each system equations (6) through (14) yields the following set of equations:

$$v_{sd} = V_s \cos \alpha_1 = r i_d + v_{rd} \quad (16)$$

$$v_{sq} = -V_s \sin \alpha_1 = r i_q + v_{rq} \quad (17)$$

$$\omega L i_d + L \frac{d}{dt} i_q = v_{rq} - v_{oq} \quad (18)$$

$$-\omega L i_q + L \frac{d}{dt} i_d = v_{rd} - v_{od} \quad (19)$$

$$v_{oq} - v_{iq} = 0 \quad (20)$$

$$v_{od} - v_{id} = d_1 v_{dcf} \quad (21)$$

$$3i_{dcf} = d_1 i_d \quad (22)$$

$$v_{iq} = d_2 \sin(\alpha_2 - \alpha_1) v_{dc} \quad (23)$$

$$v_{id} = d_2 \cos(\alpha_2 - \alpha_1) v_{dc} \quad (24)$$

$$i_{dc} = d_2 \sin(\alpha_2 - \alpha_1) i_q + d_2 \cos(\alpha_2 - \alpha_1) i_d \quad (25)$$

Using equations (16) through (25), the equivalent circuit can be reconstructed as shown in Fig. 4. Note that the resultant DQ transformed circuit is composed of LTI circuit elements and reveals the behavior characteristics without any loss of information.

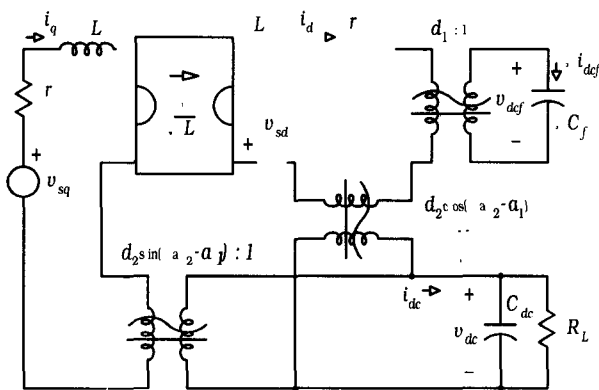


Fig. 4 Circuit DQ transformed equivalent circuit.

## IV. CONTROL CHARACTERISTICS

### A. State Equation

A transformer can be eliminated in the equivalent circuit in Fig. 4 in the following case,

$$\alpha_2 - \alpha_1 = 90^\circ \quad (26)$$

So, it can be simplified as shown in Fig. 5. The system state equation is expressed as follows:

$$\frac{d}{dt} \mathbf{x} = \mathbf{A} \mathbf{x} - \mathbf{B} \quad (27)$$

$$\mathbf{x} = [i_q \quad i_d \quad v_{dcf} \quad v_{dc}]^T \quad (28)$$

$$\mathbf{A} = \begin{bmatrix} -r/L & -\omega & 0 & -d_2/L \\ \omega & -r/L & -d_1/L & 0 \\ 0 & d_1/(3C_f) & 0 & 0 \\ d_2/C_{dc} & 0 & 0 & -1/(R_L C_{dc}) \end{bmatrix} \quad (29)$$

$$\mathbf{B} = [(V_s \cos \alpha_2)/L \quad (V_s \sin \alpha_2)/L \quad 0 \quad 0]^T \quad (30)$$

So, the system order is found to be of 4<sup>th</sup>. Control variables are  $d_1$ ,  $d_2$  and  $\alpha_2$ .

### B. DC Capacitor Voltages

In steady state operation, the inductors seem to be short and the capacitors open and all the DQ circuit variables imply DC values denoted by capital letters. Without cumbersome equation manipulations, the DC capacitor voltages can be obtained from Fig. 5 as follows

$$V_{dc} = \frac{R_L D_2 V_s \cos \alpha_2}{r + R_L D_2^2} \quad (31)$$

$$V_{dcf} = \frac{V_s}{D_1} \left( \sin \alpha_2 + \cos \alpha_2 \frac{\omega L}{r + R_L D_2^2} \right) \quad (32)$$

It is found from (31) and (32) that  $V_{dc}$  is independent of  $D_1$  while  $V_{dcf}$  is associated with both  $D_1$  and  $D_2$ . Also, it can be seen that reactance  $V_{dcf}$  is related to reactance  $\omega L$  but  $V_{dc}$  is independent of  $\omega L$ .

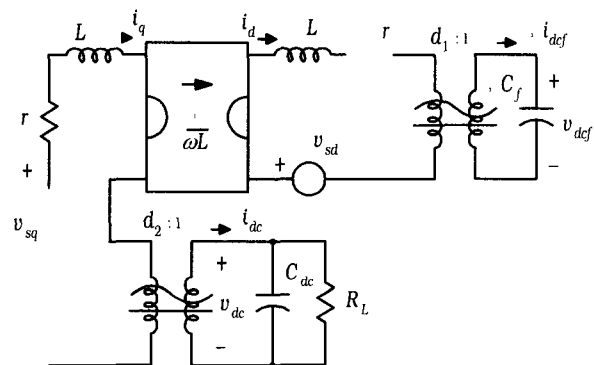


Fig. 5 The simplified circuit in the case of  $\alpha_2 - \alpha_1 = 90^\circ$ .

### C. Multilevel Output Control

The requirement for multilevel operation in (1) is very important and should be met for normal operation. That is,  $V_{dcf}$  must be half of  $V_{dc}$  in order to generate 5-level output phase voltage at the terminal of the rectifier. From (1), (31) and (32), the following important equation is obtained to remain constant ratio of  $V_{dc}$  and  $V_{dcf}$ .

$$D_1 = \frac{2}{D_2} \left[ \left( \frac{r}{R_L} + D_2^2 \right) \tan \alpha_2 + \frac{\omega L}{R_L} \right] \quad (33)$$

So, it should be noted from (26) and (33) that the only control variables for the multilevel PWM rectifier become  $D_2$  and  $\alpha_2$  and in turn  $D_1$  and  $\alpha_1$  depend on  $D_2$  and  $\alpha_2$ .

Fig. 6 shows a typical graph to figure out control range of  $D_1$  and  $D_2$  with respect to  $\alpha_2$  where the following circuit parameters are used;  $V_s=220$  V,  $r=0.7$   $\Omega$ ,  $\omega L=1.885$   $\Omega$ . As seen in Fig. 6, the modulation index  $D_2$  of TP inverter must be higher than some minimum value, in this case, about 0.15.

Fig. 7 illustrates control range of  $\alpha_2$ . Remember that the phase angle of FB inverter,  $\alpha_1$  is determined by (26). According to variable  $D_2$ , possible control range of  $\alpha_2$  is limited to some specific boundary. Especially, negative boundary of  $\alpha_2$  is narrower than positive one.

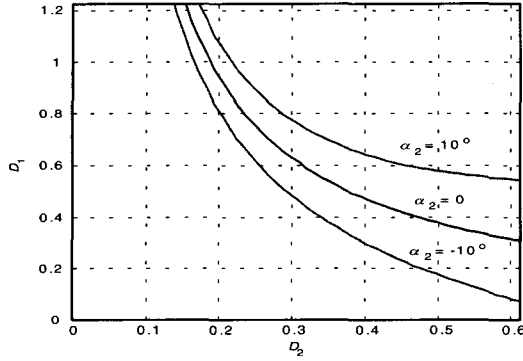


Fig. 6. Control range of  $D_1$  and  $D_2$

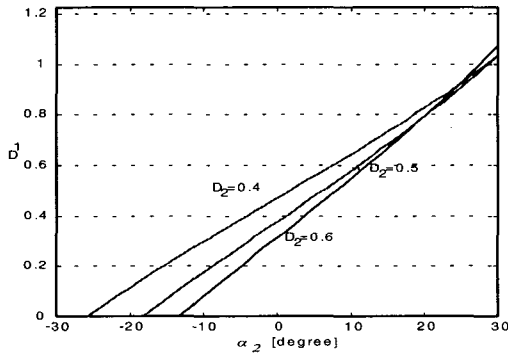


Fig. 7 Control range of  $\alpha_2$ .

#### D. Power Relationship and Unity Power Factor

Considering the only fundamental components and per-phase circuit, the power relationships in steady state operation can be obtained without difficulty. As derived in (2), (4) and (5), the source voltage and line current of phase  $a$ , become

$$V_{sa} = \sqrt{\frac{2}{3}} V_s \sin(\omega t) \quad (34)$$

$$I_a = \sqrt{\frac{2}{3}} I_q \cos(\omega t + \alpha_1) \quad (35)$$

By using the equivalent circuit of Fig. 5 in steady state, the quiescent value of  $i_q$ ,  $I_q$  can be found to be

$$I_q = \frac{V_s \cos \alpha_2}{r + R_L D_2^2} \quad (36)$$

Also, the inverter operation result in the output voltages  $V_{fa}$  and  $V_{ia}$  for FB and TP inverters respectively as follows

$$V_{fa} = \sqrt{\frac{2}{3}} D_1 V_{dcf} \sin(\omega t + \alpha_1) \quad (37)$$

$$V_{ia} = \sqrt{\frac{2}{3}} D_2 V_{dc} \sin(\omega t + \alpha_2) \quad (38)$$

So, form (34) through (38), the input real power  $P_s$  and reactive power  $Q_s$  are found to be

$$P_s = \frac{V_s^2 \cos^2 \alpha_2}{r + R_L D_2^2} \quad (39)$$

$$Q_s = \frac{V_s^2 \sin \alpha_2 \cos \alpha_2}{r + R_L D_2^2} \quad (40)$$

It can be seen form (39) and (40) that the only condition for unity power factor control is

$$\alpha_2 = 0 \quad (41)$$

Under unity power control, the real power delivered into the multilevel PWM rectifier become

$$P_s = \frac{V_s^2}{r + R_L D_2^2} \quad (42)$$

and  $P_s$  can be controlled by the magnitude modulation index of TP inverter,  $D_2$ .

Fig. 8 depicts typical variation of the delivered real and reactive powers into the rectifier with respect to  $\alpha_2$ .

#### E. Variation of DC Capacitor Voltages

In this section, the theoretical maximum values of DC capacitor voltages are discussed. The possible peak value of  $V_{dc}$  can be obtained by applying partial differentiation to (31).

$$\frac{\partial V_{dc}}{\partial D_2} = \frac{\partial}{\partial D_2} \frac{R_L D_2 V_s \cos \alpha_2}{r + R_L D_2^2} = 0 \quad (43)$$

So,  $D_{2,peak}$  which generates the maximum  $V_{dc}$ ,  $V_{dc,max}$  is found to be

$$D_{2,peak} = \sqrt{\frac{r}{R_L}} \quad (44)$$

$$V_{dc,max} = \frac{1}{2} \sqrt{\frac{R_L}{r}} \cdot V_s \cos \alpha_2 \quad (45)$$

The voltage stress at each switching devices is directly affected by the maximum value of DC capacitor voltage,  $V_{dc,max}$ , so, in the design procedure, the operating range of  $D_2$  should be carefully determined with reference to (44) and (45). Fig. 9 illustrates the DC capacitor voltages as a function of the modulation index  $D_2$  in the case of  $\alpha_2=0$ .

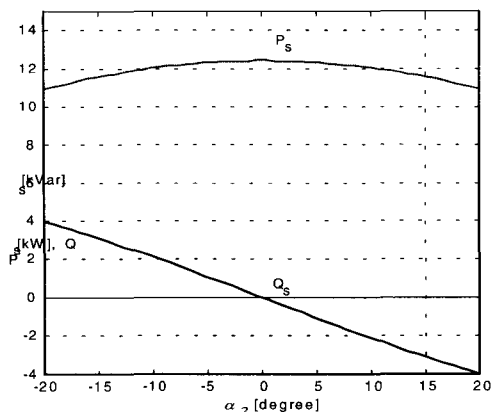


Fig. 8  $P_s$  and  $Q_s$  with respect to  $\alpha_2$ .

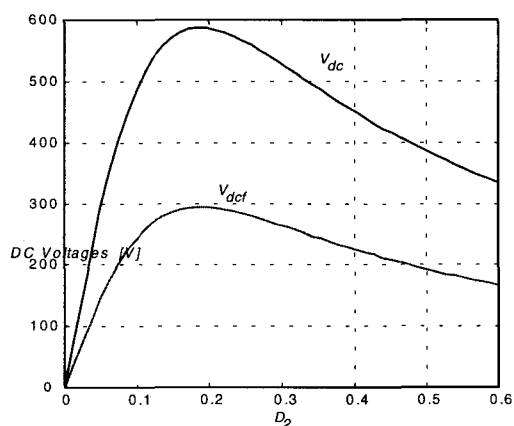


Fig. 9 Variation of  $V_{dc}$  and  $V_{dcf}$  with respect to  $D_2$ .

V. SIMULATION RESULTS

To confirm the validity of the analysis and control for the cascade multilevel rectifier, some simulations are carried out. The circuit parameters are as follows;  $V_s=220$  V,  $r=0.7 \Omega$ ,  $\omega L=1.885 \Omega$ ,  $C_f=500 \mu F$ ,  $C_{dc}=1000 \mu F$ ,  $R_L=20 \Omega$ . Also, the control is given by  $D_2=0.475$ ,  $\alpha_2=0$  and thus  $D_1=0.3968$ ,  $\alpha_1= -90^\circ$ . In the course of simulation, a simple carrier-based sinusoidal PWM is used for each FB and TP inverters in order to focus on the basic characteristics.

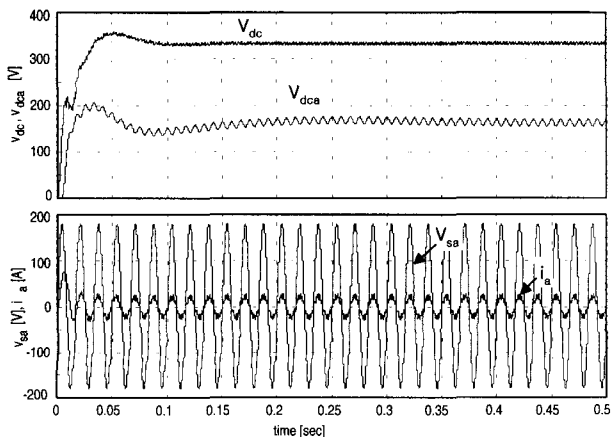


Fig. 10 Build-up procedure of DC capacitor voltages.

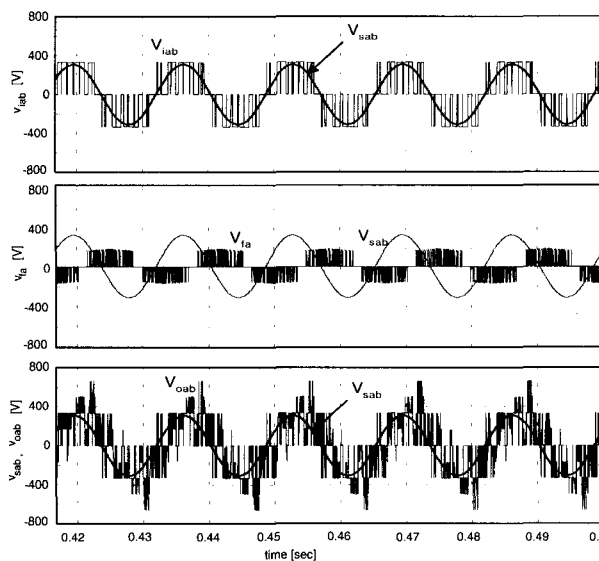


Fig. 11 Switching waveforms; (upper) line-to-line voltage of TP inverter, (middle) line-to-line voltage of FB inverter, (lower) the resultant 9-level line-to-line output voltage of the multilevel PWM rectifier.

Fig. 10 shows the open loop control characteristic during build-up of DC voltages where the rectifier goes to some steady state. The results in Fig. 4 show that  $V_{dcf}$  becomes half of  $V_{dc}$  as expected by analysis and the phase current is in phase with respect to AC source voltage and thus realizing unity power factor. Note that the ripple component of 2<sup>nd</sup> order harmonic in the DC voltage of FB inverters makes little effect on the current because of three phase symmetry operation.

Fig. 11 shows the resultant output AC voltages of FB and TP inverters. Note that the FB inverter is operated at 2160 Hz whereas the TP inverter at 540 Hz. Moreover, the output power of the FB inverter can be found to be 3.4 kVAr whereas that of the TP inverter is of 8.1 kW. So, the cascade multilevel PWM rectifier realizes the benefit of hybrid structure. Actually, the FB inverters take charge of supplying the only reactive power and the TP inverter absorbs the only active power.

VI. CONCLUSION

This paper presents a transformerless cascade multilevel PWM rectifier with unity input power factor. The features and advantages of the proposed PWM rectifier can be summarized as follows;

- 1) It realizes the high power and high voltage AC/DC power conversion owing to multilevel structure,
- 2) It uses no transformer which is bulky, heavy and even expensive,
- 3) It has hybrid structure so that semiconductor devices can be effectively utilized,
- 4) It produce high quality AC current even in high power and high voltage applications,
- 5) The input power factor remains unity by simple modulation index control.

## REFERENCES

- [1] J. W. Dixon, A. B. Kulkarni, M. Nishimoto and B. T. Ooi, "Characteristic of a controlled-current PWM rectifier-inverter link", IEEE trans. on Industry Applications, Vol. 23, No. 1, pp. 78-84, 1987.
- [2] C. T. Rim, N. S. Choi, G. C. Cho and G. H. Cho, "A Complete DC and AC Analysis of Three-Phase Controlled-Current PWM Rectifier Using Circuit D-Q Transformation", IEEE trans. on Power Electronics, Vol. 9, No. 4, 1994.
- [3] N. S. Choi, Jung G Cho and Gyu H. Cho, "A general circuit topology of multilevel inverter", IEEE PESC Record pp. 96-103, 1991.
- [4] F. Z. Peng, J.-S. Lai, J. W. McKeever and J. VanCoevering, "A Multilevel Voltage -Source Inverter with Separate DC Sources for Static Var Generation", IEEE trans. on Industry Applications, Vol. 32, No. 5, pp. 1130-1138, 1996.
- [5] Frank Schettler, "Device for Increasing the Power Yield of the Fundamental Component of a Self-Commutated Power Inverter", United States Patent, Patent Number 5673189, 1997.
- [6] M. D. Manjrekar, P. Steimer and T. A. Lipo, "Hybrid Multilevel Power Conversion System: a Competitive Solution for High Power Applications", IEEE IAS Annual Meeting Conference Records, pp. 1520-1527, 1999.
- [7] N. S. Choi, Cuk C. Cho and Gyu H. Cho, "Modelling and analysis of multilevel voltage source inverter applied as a static var compensator", International Journal of Electronics, Vol. 75, No. 5, pp. 1015-1034, 1993.

**Nam-Sup Choi**

Received the B.S. degree in electrical engineering from Korea University, Seoul, Korea, in 1987, and the M.S. and PhD degree in power electronics from Korea Advanced Institute of Science and Technology(KAIST), Taejeon, Korea, in 1989 and 1994, respectively. He is currently an associate professor of department of electrical engineering, Yosu National University in Yeosu, Korea. Dr. Choi is a member of the KIMICS.